# A Numerical Study of Low Grazing Angle Backscattering from Random Rough Surfaces

# 不規則 粗面에서 저입사각 후방산란에 관한 수치해석

Kwang-Yeol Yoon

윤 광 렬

## Abstract

We have numerically analyzed the electromagnetic wave scattering from randomly rough dielectric surfaces by using the finite volume time domain (FVTD) method. We have then shown that the present method yields a reasonable solution even at low-grazing angle (LGA). It should be noted that the number of sampling points per wavelength should be increased when more accurate numerical results are required, which fact makes the computer simulation impossible at LGA for a stable result. However, when the extrapolation is used for calculating the scattered field, an accurate result can be estimated. If we want to obtain the ratio of backscattering between the horizontal and vertical polarization, we do not need the large number of sampling points. The results are compared with the experimental data.

Key words : FVTD Method, Low Grazing Angle, Backscattering Coefficient, Polarization Ratio

## 요 약

맥스웰방정식의 직접해인 FVTD(Finite Volume Time Domain)법을 이용하여, 低入射時의 不規則 粗面에서의 전자파 산란 문제를 수치해석 하였다. FVTD법은 복잡한 구조의 전자파의 산란문제에 대해서 개발된 시간영역에의한 수치해석법이며, 從來의 FDTD(Finite Difference Time Domain)법 보다 임의형태의 경계문제를 쉽게 다룰 수 있는 利點을 가지고 있다. 그러나 산란물체의 형태가 아주 복잡하고 精度를 문제 삼을 경우 FVTD법에서는 셀 사이즈(cell size)를 충분히 細分化할 필요가 있다. 그 경우 셀 사이즈에 의한 數値解의 收束性을 檢討하고, 外插法(extrapolation method)을 이용해서 간단하고 정확한 후방산란계수를 推定하는 方案을 제시했다. 더우기 취급하는 偏波의 相異를 特徵짓는 레이다 단면적의 偏波比에 대해서, 입사각(grazing angle) 이 10度 이하의 海面 레이다의 실험결과와 비교하여, FVTD법의 수치계산 결과가 實測値와 잘 일치하는 결과를 提示했다.

## Ⅰ. Introduction

Numerical solution techniques play an increasingly important role in understanding and predicting scattering from randomly rough surfaces. An exact analytical solution for random rough surfaces does not exist. However, the classical approximate analytical solutions exist for rough surfaces with specific types of surface roughness conditions. The perturbation method applies to a slightly rough whose root mean square (rms) height is smaller than the wavelength[1],[2]. The Kirchhoff approximation is

「The present research has been conducted by the Bisa Research Grant of Keimyung University in 2002.」

계명대학교 공학부 전자공학과(Department of Electronic Engineering, Keimyung University)

· 논 문 번 호 : 20020401-043
· 수정완료일자 : 2002년 5월 1일

applicable to a surface whose radius of curvature is much greater than the wavelength[3]. In contrast to classical approaches, the small-slope approximation (SSA) of Voronovich[4] is valid to only the roughness of small slope. These are limited surface roughness conditions.

In the numerical approaches with the remarkable progress of computer, the integral equation (IE) techniques[5],[6], finite-difference time-domain (FDTD) and finite-volume time-domain (FVTD) method[7]~[9] are shown to be useful for solving various problems of electromagnetic wave scattering from rough surfaces. These numerical methods are based on the wave theory. In this context, numerical methods seem to be well suited to the rough surface scattering in the case of LGA. However, numerical methods encounter difficulties at LGA because of the limitation of computer resources. The incident wave propagates repeating multiple scattering along the rough surface at LGA and hence we need to analyze such a long propagation.

Over the past few years, we have developed the FVTD technique for the problem of the wave scattering from lossy dielectric random rough surfaces. We have found that questions regarding the stability of solution with respect to sampling points per wavelength exist[9]. In order for a numerical computation to yield accurate results, the sampling intervals should be taken to be much smaller than the wavelength. As a result, it is difficult to compute accurate results for the LGA from rough surface scattering in particular, because the computer resources are limited. It is recently reported that the IE technique has not reached a stable solution for randomly rough perfectly conducting surface by using very short sampling interval and therefore needs the curvature terms which are proportional to the surface curvature at each point to obtain a stable result[5].

The purpose of this paper is to develop an exact numerical FVTD technique and to provide the highly accurate numerical results for the problem of wave scattering from lossy dielectric randomly rough surfaces. We have found some important numerical stability with respect to the sampling points, which can be provided to estimate an accurate solution by extrapolation. This finding prompted us to make a more accuracy how the FVTD method is performed, and what the role of the number of sampling point is. The geometry of problem is shown in Fig. 1.

## Ⅱ. FVTD Formulation

In FVTD formulation, the Maxwell equations are discretized on the basis of the volume integration with respect to a small cell. In the Cartesian coordinate system FVTD is equivalent to the conventional FDTD. In order to apply to the inhomogeneous electromagnetic problems, FVTD employs averaged medium constants in each cell[10]. Recently, it is reported that FDTD has also used the same procedure with the averaged or effective

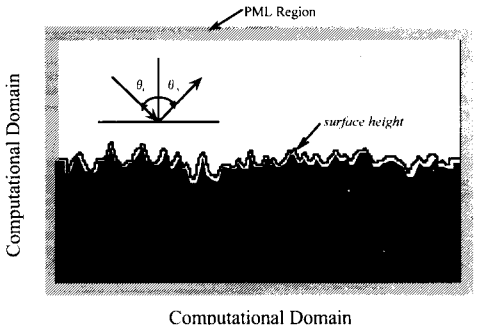


Fig. 1. Problem geometry including FVTD computational grid.

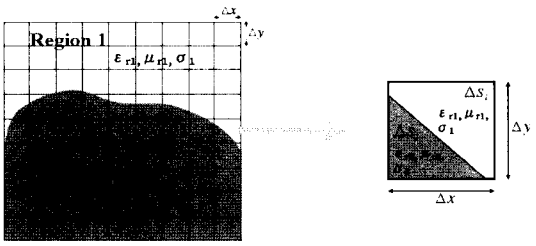


Fig. 2. Approximation of general boundary Region 1 and Region 2 for arbitrary shaped surface.

material parameters[11]. Now we consider an arbitrarily shaped boundary between two different electric and magnetic materials. One material is denoted by the constants with $\varepsilon_{rl} = \mu_{rl} = 1.0$ and $\sigma_1 = 0$, and the other is designated by the constants ($\varepsilon_{r2}$, $\mu_{r2}$, $\sigma_1$). We assume that one part of the $(i,j)$-th cell is occupied by the former material with area Region 1 and the other part is occupied by the latter material with area Region 2 as shown in Fig. 2. Then we can approximately evaluate the material constants in the $(i,j)$-th cell in an average fashion as follows:

$$\varepsilon_r' = \frac{\varepsilon_{r1}\Delta S_1 + \varepsilon_{r2}\Delta S_2}{\Delta S} \tag{1}$$

$$\mu_r' = \frac{\mu_{r1}\Delta S_1 + \mu_{r2}\Delta S_2}{\Delta S} \tag{2}$$

$$\sigma' = \frac{\sigma_1\Delta S_1 + \sigma_2\Delta S_2}{\Delta S} \tag{3}$$

where

$$\Delta S = \Delta S_1 + \Delta S_2 = \Delta x \Delta y \tag{4}$$

Now we summarize the FVTD formulations. For computational reason, magnetic field is normalized by the intrinsic impedance of free space in this paper. We assign the averaged dielectric constant $\varepsilon_{rij}$, electric conductivity $\sigma_{ij}$ in each cell. Then we can define the averaged and discretized electric field $E_n(i,j)$ in the $(i,j)$-th cell and in the $n$-th time point. Similarly we have the magnetic field $H^{n'}(i,j)$ in the $n'$-th time point where $n'=n-1/2$.

With these notations the FVTD equations for horizontal polarization are expressed as follows[10]:

$$H_x^{n+1}(i,j) = \Xi^{i,j} H_x^n(i,j) - \Gamma_y^{i,j} A^{i,j}[E_z^n(i,j+1) - E_z^n(i,j-1)] \tag{5}$$

$$H_y^{n+1}(i,j) = \Xi^{i,j} H_y^n(i,j) - \Gamma_x^{i,j} A^{i,j}[E_z^n(i+1,j) - E_z^n(i-1,j)] \tag{6}$$

$$E_z^{n+1}(i,j) = \Omega^{i,j} E_z^n(i,j) - \Gamma_y^{i,j} B^{i,j}[H_x^{n+1}(i,j+1) - H_x^{n+1}(i,j-1)] + \Gamma_x^{i,j} B^{i,j}[H_y^{n+1}(i+1,j) - H_y^{n+1}(i-1,j)] \tag{7}$$

The FVTD equations for the vertical polarization are expressed as follows [10]:

$$H_z^{n+1}(i,j) = \Xi^{i,j} H_z^n(i,j) - \Lambda_y^{i,j} A^{i,j}[E_x^n(i,j+1) - E_x^n(i,j-1)] + \Lambda_x^{i,j} A^{i,j}[E_y^n(i+1,j) - E_y^n(i-1,j)] \tag{8}$$

$$E_x^{n+1}(i,j) = \Omega^{i,j} E_x^n(i,j) + \Gamma_y^{i,j} B^{i,j}[H_z^{n+1}(i,j+1) - H_z^{n+1}(i,j-1)] \tag{9}$$

$$E_x^{n+1}(i,j) = \Omega^{i,j} E_x^n(i,j) + \Gamma_x^{i,j} B^{i,j}[H_z^{n+1}(i+1,j) - H_z^{n+1}(i-1,j)] \tag{10}$$

The step parameters used above are defined by

$$\Xi^{i,j} = \exp(-\alpha_{mi,j}) \tag{11a}$$

$$\Lambda_{x,y}^{i,j} = \frac{c\Delta t}{2\mu_{ri,j}\Delta x, y} \tag{11b}$$

$$A^{i,j} = \frac{1-\exp(-\alpha_{mi,j})}{\alpha_{mi,j}} \tag{11c}$$

$$\Omega^{i,j} = \exp(-\alpha_{i,j}) \tag{11d}$$

$$\Gamma_{x,y}^{i,j} = \frac{c\Delta t}{2\varepsilon_{ri,j}\Delta x, y} \tag{11e}$$

$$B^{i,j} = \frac{1-\exp(-\alpha_{i,j})}{\alpha_{i,j}} \tag{11f}$$

$$\alpha_{mi,j} = \frac{\sigma_{mi,j}\Delta t}{\mu_0 \mu_{ri,j}} \tag{11g}$$

$$\alpha_{i,j} = \frac{\sigma_{i,j}\Delta t}{\varepsilon_0 \varepsilon_{ri,j}} \tag{11h}$$

where $\Delta x$ and $\Delta y$ are the spatial increment and $\Delta t$ is the time difference. Moreover, $c = 1/\sqrt{\varepsilon_0 \mu_0}$ is the light velocity in free space.

In the FVTD computation we have assumed the incident wave to be a modified Gaussian beam [3] as follows:

$$F_z^i(x,y) = \exp\{-jk(x\sin\theta_i - y\cos\theta_i)[1+w(x,y)] \cdot \exp\{-(x+y\tan\theta_i)^2/g^2\} \tag{12}$$

where $F_z^i$ is either the $E_z^i$ or $H_z^i$ field, depending on the polarization considered. In (12) the $\theta_i$ is the grazing angle of incident wave, $k = 2\pi/\lambda$ is wave

number in free space and where $\lambda$ is the electromagnetic wavelength in free space. Moreover,

$$w(x,y)=\frac{2(x+y\tan\theta_i)^2/g^2-1)}{(kg\cos\theta_i)^2} \tag{13}$$

where $g$ is the parameter that controls the tapering and gives an acceptable tapering at the edges.

## Ⅲ. Far-Field Conversion and Scattering Cross Section

FVTD allows us to compute near field data in the time domain just inside the perfectly matched layer (PML) region[12], and thus the near-field data in the spectral domain are given by performing discrete Fourier transform. As a result, far-field data can be calculated by the Kirchhoff-Huygens principle. The usual derivation procedure for near-field to far-field transformations starts with the surface equivalence theorem from which the equivalent electric and magnetic currents can be extracted on a surface enclosing the scattering object. The scattered field in the far-field can be derived by integrating the equivalent currents multiplied with a free space Green's function[13]. In this study, we treat the FVTD method for a two-dimensional scattering problem with a one-dimensional rough surface as shown in Fig. 3. For vertical polarization we obtain for magnetic scattered field as

$$H_z^s=-jk\frac{e^{-j(kr+\pi/4)}}{\sqrt{8\pi kr}}\int_{-L_x}^{L_x}[-H_z(x,L_y)\sin\theta_s+E(x,L_y)]dx \times\exp(jk(x\cos\theta_s+L_y\sin\theta_s)) \tag{14}$$

and for horizontal polarization the electric scattered field can be given by

$$E_z^s=-jk\frac{e^{-j(kr+\pi/4)}}{\sqrt{8\pi kr}}\int_{-L_x}^{L_x}[-E_z(x,L_y)\sin\theta_s+H_x(x,L_y)]dx \times\exp(jk(x\cos\theta_s+L_y\sin\theta_s)) \tag{15}$$

where $E_z(x,L_y)$, $H_x(x,L_y)$, $H_z(x,L_y)$, and $E_x(x,L_y)$ are field values on the horizontal portion of the dashed path in Fig. 3. Along the dashed path in this figure

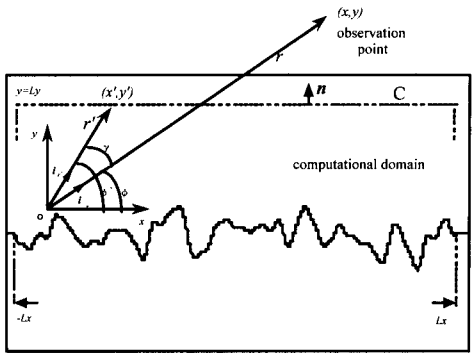


Fig. 3. Computational domain in which the scattered field propagate.

phasor quantities for $E_z$, $H_x$, $H_z$ and $E_x$ are obtained from the FVTD algorithm.

The bistatic normalized radar cross section (NRCS) is defined by [7] as follows:

$$\sigma^0(\theta_i,\theta_s)=\lim_{r\to\infty}\frac{2\pi r\left|F_z^s\right|^2}{\int\left|F_z^i(x,0)\right|^2dx} \tag{16}$$

where $F_z^s$ is given by $F_z^s=H_z^s$ for vertical polarization and $F_z^s=E_z^s$ for horizontal polarization. The backscattered NRCS is as follows:

$$\sigma_{bsc}^0(\theta_i)=\sigma^0(\theta_i,-\theta_i) \tag{17}$$

The scattering coefficient $\gamma^0$ is defined in terms of the projected area of the incident wave [13]:

$$\gamma^0(\theta_i,\theta_s)=\lim_{r\to\infty}\frac{2\pi r\left|F_z^s\right|^2}{\cos\theta_i\int\left|F_z^i(x,0)\right|^2dx} \tag{18}$$

Thus we have

$$\sigma^0(\theta_i,\theta_s)=\cos\theta_i\,\gamma^0(\theta_i,\theta_s) \tag{19}$$

For the random rough surface the NRCS is averaged over an ensemble of finite surface realizations to obtain an ensemble average of *NRCS* $<\sigma^0(\theta_i,\theta_s)>$. According to the computational procedures described above, we can obtain the scattered far fields for two different polarizations,

$\sigma^0_{(hh)}$ and $\sigma^0_{(vv)}$, for one rough surface profile. Then we can calculate the averaged backscattering ratio of the horizontal to vertical polarizations as follows:

$$R_{(hh/vv)} = \frac{<\sigma^0_{(hh)}>}{<\sigma^0_{(vv)}>} \tag{20}$$

## Ⅳ. Numerical results

In the numerical simulation, the relative permittivity of soil at soil moisture of 15% are chosen as $\varepsilon_{r2}$= 10.8, $\mu_{r2}$= 1.0 and $\sigma_2$= 0.106 (S/m) at L band (1.43 GHz)[6]. We consider the rms slope angles of the Gaussian random rough surfaces. The rms slope $s$ is defined by as follows:

$$s = \sqrt{2}\frac{h}{l} = \tan\gamma \tag{21}$$

where $h$ denotes the rms height, $l$ is the correlation length, and $\gamma$ is the rms slope angle.

### 4-1 Convergence with Respect to the Number of Sampling Points

First, we consider the convergence of numerical solution with respect to sampling points per wavelength. In order for a numerical computation to yield accurate results, the sampling intervals should be taken to be much smaller than the wavelength. To make sure the accuracy of computation, we need to check the numerical convergence of backscattering coefficients by changing the number of sampling points per wavelength as follows;

$$\Delta x = \Delta y = \frac{\lambda}{N} \ (N=20,\ 40,\ 80,\ 160) \tag{22}$$

where $\lambda$ is the wavelength in free space. Increasing the number, we can estimate an accurate value by extrapolation based on Lagrange's method[14]. To do this, we express $f(x)$ in the following form:

$$f(x) = \sum_{j=1}^{m} f(x_i)\frac{F(x)}{(x-x_i)(F'(x_j)} \tag{23}$$

where

$$F(x) = \prod_{j=1}^{m}(x-x_j) = (x-x_1)(x-x_2)\cdots(x-x_m) \tag{24}$$

$$F'(x) = \frac{dF(x)}{dx} \tag{25}$$

For the incident angle of 80°, the surface length $L$ is selected as 102.4 $\lambda$, and the tapering parameter in this case is $g = L/4$ to ensure that the effects of edge diffraction can be neglected for the incident and scattering angles of interest. An example of results calculated with COMPAQ ALPHA STATION XP 1000 is shown in Table 1 where the CPU time and memory requirements for one realization are tabulated to show roughly the scale of computation.

Fig. 4 shows the backscattering coefficients from six realizations of random rough lossy dielectric surfaces whose rms slope angle $\gamma$ is all 25.2°. Note that some results have not reached the extrapolated value even at sampling points of 160. Because the average of backscattering coefficients is required in random rough surface scattering, we take the average for 50 surface realizations. As a result, Fig. 5 shows that even for the sampling points of 160 the backscattering coefficient still has not reached its final value and that we need larger number of sampling points to obtain accurate solutions. If, however, extrapolation is used for calculating the backscattering coefficient, an accurate solution is easily obtained because the numerical results show a good convergence as shown in Fig. 5.

Next it is of interest to examine what occurs as the correlation length increases for a fixed $h$. This is

Table 1. The CPU time and memory requirements for one realization.

| Cell size($1/\lambda$) | CPU time (sec) | Memory (Mbytes) |
|---|---|---|
| 1/20 | 35.73 | 7.6 |
| 1/40 | 263.15 | 26.1 |
| 1/80 | 1630.32 | 55.9 |
| 1/160 | 14901.46 | 183.7 |

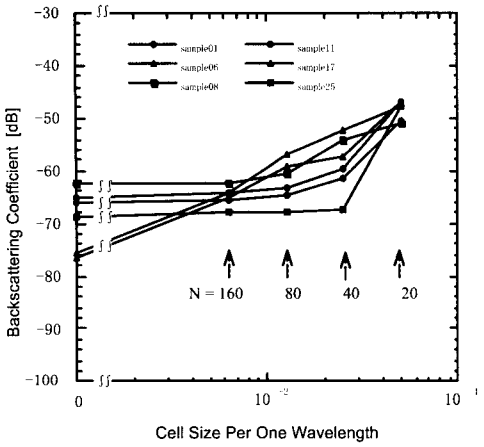


Fig. 4. Comparison of the variation of backscattering coefficients with respect to the number of sampling points per wavelength in case of single realization of Gaussian surface for $h = 0.2\lambda$, $l = 0.6\lambda$, $\gamma$=25.2°.

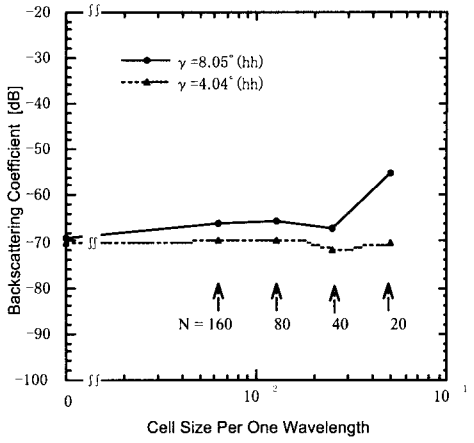


Fig. 6. Convergence with respect to the number of sampling points per wavelength in case of 50 realizations of Gaussian small-slope surface.

equivalent to decreasing the rms slope angle for a fixed $h$. In Fig. 6, we have used the correlation length of 2.0 $\lambda$ and 4.0 $\lambda$. The comparison between Figs. 4 and 5 shows effects of decreasing rms slope angles from 25.2° to 4.02° for a fixed $h$. For small slope surfaces, the stable result is obtained at sampling points of 40 when the correlation length is

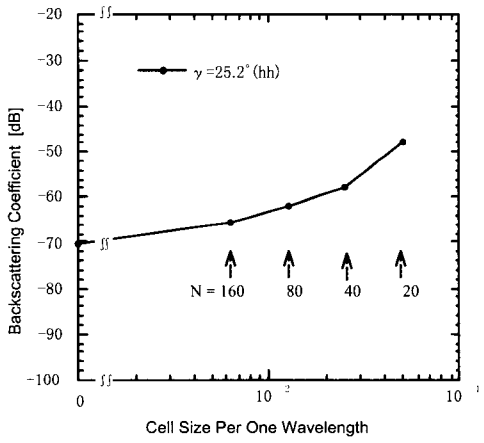


Fig. 5. Comparison of the variation of backscattering coefficients with respect to the number of sampling points per wavelength in case of 50 realizations of Gaussian surface for $h = 0.2\lambda$, $l = 0.6\lambda$, $\gamma = 25.2°$.

larger than the wavelength for a fixed $h$. In other words, the backscattering coefficient converges fast when the surface correlation length is larger than the wavelength, as shown in Fig. 6. However, the backscattering coefficient converges slowly when the surface correlation length is smaller than the wavelength, as shown in Fig. 5.

Moreover, we plot the horizontal and vertical polarization backscattering in Fig. 7 by using the same roughness as used in Fig. 5. It should be emphasized from Fig. 7 that the backscattering ratios of two different polarizations is numerically stable. The difference between the ratio at sampling points 160 and 20 is only 1.5 dB. This result suggests that the sampling points of 20 are enough for calculating the ratio of backscattering.

To summarize these results, it was demonstrated that many sampling points per wavelength should be used when accurate numerical results are needed for large-slope surfaces. In other words, it is difficult to compute accurate results for the LGA scattering on rough surfaces of various roughness parameters. Other methods such as IE technique have also the same difficulty[5]. If, again, extrapolation is used for

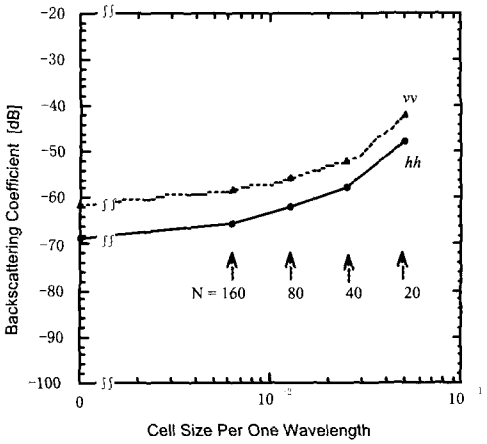


Fig. 7. Comparison of backscattering coefficients with respect to the number of sampling points per wavelength in case of 50 realizations of Gaussian large-slope surface for horizontal and vertical polarization.

calculating the backscattering coefficient, a more accurate solution is easily estimated because the numerical results show a good convergence as shown in Fig. 7. We emphasize that the use of the FVTD and extrapolation method does not need troublesome analytic treatments such as the estimate of curvature terms at each surface point used in [5].

### 4-2 Comparison with Experimental Data

We compare the presented numerical results with experimental data of the reference [15] for the ratio of backscattering cross sections between horizontal and vertical polarizations. The accuracy of the FVTD method when compared with experiment depends on many factors, such as the angles of incidence and the surface statistics. The material constants of the rough surface are selected to simulate seawater as $\varepsilon_{r2}$ = 51.4, $\mu_{r2}$ = 1.0 and $\sigma_2$ = 21.75($S/m$) at $X$ band (10.0 GHz)[35]. This approximation is reasonable since seawater is a fairly high-loss medium at microwave frequencies. We use many different types of the Gaussian randomly rough surfaces. We chose the cell size as $\Delta x = \Delta y = \lambda/20$ and it is enough for calculating the ratio of two different polarizations as mentioned in Section 4-1. For incident angles up to 70°, we use 200 $\lambda$ surfaces, but we increase this value to 500 $\lambda$ for incident angles up to 80°.

In Figs. 8 and 9, the polarization ratio calculated from in the Appendix (A1) by the SPM for a lossy dielectric surface is evaluated and plotted as a function of incident angle (solid line). Also plotted is the polarization ratio calculated from in the Appendix (A2) by the SPM for a perfect conducting surface (dashed line), and the experimental data (squares) from reference[35]. Of course the FVTD results are plotted in these figures. The SPM result agrees with the experimental data at incident angles smaller than 70° when the appropriate dielectric constant is used[15]. At incident angles of more than 70°, however, the SPM result begins to deviate from the experimental data. In the FVTD simulations using roughness parameters such as $h$ = 0.2$\lambda$ , $l$ = 5.0$\lambda$ (solid circles), the results are almost in good agreement over incident angles between 20° and 80° with experimental data[15]. We also show the ratio of backscattering cross sections between two polarizations at incident angles of more than 80° in Fig. 9.

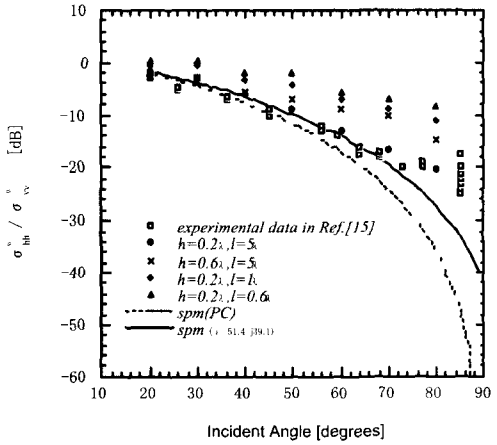


Fig. 8. The ratio of backscattering cross section between two polarizations and comparison among the FVTD, SPM and Experimental data [35] in case of $\theta_i \leq 80°$, $L$=200 $\lambda$, and the ensemble average for 50 surfaces.

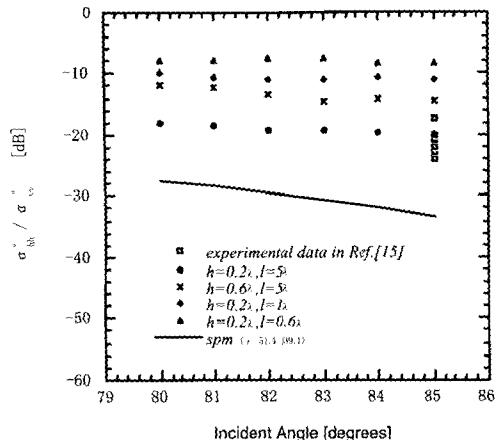


Fig. 9. The ratio of backscattering cross section between two polarizations and comparison among the FVTD, SPM and Experimental data [35] in case of $\theta_i \leq 80^\circ$, $L=500\,\lambda$, and the ensemble average for 50 surfaces.

It is shown that both results of experiment and simulation with $h=0.2\,\lambda$ and $l=5.0\,\lambda$ are in substantial agreement at incident angle of 85° and that the SPM result gives much smaller ratio than the FVTD numerical simulations.

## V. Conclusion

The electromagnetic waves scattering from random rough lossy dielectric surfaces are numerically analyzed by using the finite-volume time-domain method. It is shown that the present method yields a reasonable solution even at low-grazing-angle (LGA) backscattering. On the FVTD solution, we found some important results for the numerical convergence with respect to the sampling points. The backscattering coefficient converges fast when the surface correlation length is larger than the wavelength, while it converges slowly when the surface correlation length is smaller than the wavelength. The number of sampling points per wavelength should be increased when more accurate numerical results are required, which fact suggests that the computer simulation becomes difficult at LGA. However, when the extrapolation is used for calculating the scattered field, an accurate result can be estimated. Moreover, for calculating the polarization ratio of backscattering cross sections, we do not need the large number of sampling points. These results show that the number of sampling points required to give a good accuracy depends on the observation target. In addition, it is indicated that the FVTD results are in good agreement with the experimental data.

## Appendix

When a plane wave is incident on a random rough surface of complex dielectric constant at an angle, Rice[2] derived by the small perturbation method (SPM) the formulas that led to the average cross section per unit area for horizontally and vertically polarized backscatter from the surface[3]. They are given by

$$\sigma^0_{hh}(\theta_i) = 4\pi k^4 \cos^4\theta_i \left| \frac{(\varepsilon-1)}{[\cos\theta_i + (\varepsilon - \sin^2\theta_i)^{1/2}]^2} \right|^2 W(2k\sin\theta_i, 0) \tag{A1-a}$$

for horizontal polarization and

$$\sigma^0_{vv}(\theta_i) = 4\pi k^4 \cos^4\theta_i \left| \frac{(\varepsilon-1)[\varepsilon(1+\sin^2\theta_i)-\sin^2\theta_i]}{[\cos\theta_i + (\varepsilon - \sin^2\theta_i)^{1/2}]^2} \right|^2 W(2k\sin\theta_i, 0) \tag{A1-b}$$

for vertical polarization where $k = 2\pi/\lambda$ is the wave number in free space, and $W(\cdot)$ is the two-dimensional wave number spectral density of the surface roughness. For a perfectly conducting surface, there are

$$\sigma^0_{hh}(\theta_i) = 4\pi k^4 \cos^4\theta_i\, W(2k\sin\theta_i, 0) \tag{A2-a}$$

and

$$\sigma^0_{vv}(\theta_i) = 4\pi k^4 (1+\sin^2\theta_i)^2\, W(2k\sin\theta_i, 0) \tag{A2-b}$$

## References

[1] S. O. Rice, "Reflection of electromagnetic wave from slightly rough surfaces", *Commun. Pure Appl. Math.*, vol. 4, pp. 351-378, 1951.

[2] G. R. Valenzulea, J. W. Wright and J. C. Leader, "Comments on 'The relationship between the Kirchoff approach and small perturbation analysis in rough surface scattering theory", *IEEE Trans. Antennas Propagat.*, vol. AP-20, pp. 536-539, July 1972.

[3] E. I. Thoros, "The validity of the Kirchhoff approximation for rough surface scattering using a Gaussian roughness spectrum", *J. Acoust. Soc. Am.*, vol. 83, no. 1, pp. 78-92, Jan. 1988.

[4] Alexander G. Voronovich, *Wave Scattering from Rough Surfaces (Springer series on Wave Phenomena)*, 2nd edition Springer-Verlag Berlin Heidelberg New York, 1999.

[5] J. V. Toporkov, R. T. Marchand and G. S. Brown, "On the discretization of integral equation describing scattering by rough conducting surface", *IEEE Trans. Antennas Propagat.*, vol. 46, no. 1, pp. 150-161, Jan. 1998.

[6] C. H. Chan, L. Tsang and Q. Li, "Monte Carlo simulations of large-scale one-dimensional random-rough surface scattering at near-grazing incidence: penetrable case", *IEEE Trans. Antennas Propagat.*, vol. 46, no. 1, pp. 142-149, Jan. 1998.

[7] F. D. Hastings, J. B. Schneider and S. L. Broschat, "A Monte-Carlo FDTD technique for rough surface scattering", *IEEE Trans. Antennas Propagat.*, vol. 43, no. 11, pp. 1183-1191, Nov. 1995.

[8] K. Uchida, K. Y. Yoon, Y. Kuga and A. Ishimaru, "FVTD analysis of electromagnetic wave scattering by rough surface", *IGARSS'98*, vol. IV, DD Ⅱ, pp. 2292-2294, July 1998.

[9] K. Y. Yoon, M. Tateiba and K. Uchida, "FVTD Simulation for Random Rough Dielectric Surface Scattering at Low Grazing Angle", *IEICE Trans. Electron.*, vol, E83-C. Dec. 2000.

[10] K. Uchida, T. Matunaga, T. Noda and K. K. Han, "FVTD algorithm and its application procedure", *Res. Bull. Fukuoka Inst. Tech.*, vol. 29, no. 1, pp. 121-130, Oct. 1996.

[11] G. Marrocco, M. Sabbadini and F. Bardati, "FDTD Improvement by Dielectric Subgrid Resolution", *IEEE Trans. on MTT*, vol. 46, no. 12, pp. 2166-2169, Dec. 1998.

[12] J. P. Berenger, "A perfectly matched layer for the absorption of electromagnetic waves", *J. Comp. Phys.*, vol. 114, no. 2, pp. 185-200, Oct. 1994.

[13] A. Ishimaru, *Electromagnetic Wave Propagation, Radiation, and Scatterimg*, Prentice-Hall, Inc. 1991.

[14] A. Ishimaru, *Wave Propagation and Scattering in Rabdom Media*, IEEE PRESS, New York, 1997.

[15] P. H. Y. Lee, J. D. Bater, K. L. Beach, C. L. Hindman, B. M. Lake, H. Rungaldier, J. C. Shelton, A. B. Williams, R. Yee and H. C. Yuen, "X band microwave backscattering form ocean waves", *J. Geophysical Res.*, vol. 100, no. C2, pp. 2591-2611, Feb. 15, 1995.

윤 광 렬

1994년 3월: 일본 후쿠오카 공업대학교 정보공학과 (공학사)
1996년 3월: 일본 후쿠오카 공업대학교 대학원 공학연구과 정보통신전공 (공학석사)
2001년 3월: 일본 큐슈대학교 시스템 정보과학연구과 정보통신전공 (공학박사)
2001년 4월~2001년 8월: 큐슈대학교 시스템 정보과학연구원 연구원
2001년 9월~현재: 계명대학교 공학부 전자공학과 전임강사
[주 관심분야] 전자파이론, 전파전파, 수치해석